

in the decays of Er^{171} and Er^{169} . So level F is tentatively assigned to spin and parity $\frac{7}{2}^-$. Then the β transition from ground level of Er^{173} ($\frac{5}{2}^-$ [5,1,4]) to this level is allowed transition, ($\Delta K=0$, N_0), although it is Λ forbidden ($\Delta\Lambda=1$, $\Delta n_z=-1$, $\Delta N=0$).

The γ transition from this level to $K=\frac{1}{2}$ rotational bands will be highly K forbidden since $\Delta K=3$, and hence it is expected that this level is a retarded state. The results obtained in γ - γ coincidence measurement seem to agree with this. However, due to the very low activity we could not perform any measurement to determine the lifetime of this state. We have not made assignments of spin and parity of the higher levels, because of the very low intensities of the γ rays.

I. Cross Section of the $\text{Yb}^{176}(n,\alpha)\text{Er}^{173}$ Reaction

The cross section for 14.8-MeV neutron-induced (n,α) reaction on Yb^{176} was calculated to be 0.20 ± 0.05 mb using the cross-section values of (n,p) and ($n,2n$) reactions on Yb^{176} .^{1,2} The following equation was used for this calculation:

$$\sigma(n,\alpha) = \sigma_i A_{173}^0 (1 - e^{-\lambda_i t}) / A_i^0 (1 - e^{-\lambda_{173} t}),$$

where σ_i are the cross section for (n,p) and ($n,2n$) reactions, λ_i are the decay constants of the corresponding nuclei, Tm^{176} and Yb^{175} , respectively, A_{173}^0 and A_i^0 are

the activities of the nuclei Er^{173} , Tm^{176} , and Yb^{175} at the end of bombardment, and t is the duration of irradiation.

Bramlitt and Fink¹⁵ have reported that the cross section should be corrected for the effect of the decay of the neutron flux during the irradiation. Using the method given by Bramlitt and Fink and $t_{1/2} \approx 2.5$ h for the decay of the neutron flux, the correction factors σ_s'/σ_s were calculated to be 1.09 when Yb^{175} was used as the monitor and 0.92 when Tm^{176} was used as the monitor. These values were within the experimental error of the value σ_s , calculated from the constant flux during the irradiation, because of the low activity of the sample and of the short duration of the irradiation. The cross-section values of (n,α) reaction calculated from (n,p) and ($n,2n$) reaction cross sections agreed within experimental error.

ACKNOWLEDGMENTS

The authors would like to express their deep appreciation to Professor P. K. Kuroda for his advice and encouragement. We are also very grateful to Dr. J. L. Meason for valuable suggestions and comments. The authors would also like to thank P. H. Pile for the operation of the accelerator and D. E. Baker for technical assistance.

¹⁵ E. T. Bramlitt and R. W. Fink, *Phys. Rev.* **131**, 2649 (1963).

Resonance Analysis of the ^{233}U Fission Cross Section*†

D. W. BERGEN AND M. G. SILBERT

University of California, Los Alamos Scientific Laboratory, Los Alamos, New Mexico

(Received 28 August 1967)

The neutron-induced fission and capture cross sections of ^{233}U were measured by time of flight with a nuclear detonation as the neutron source. Cross-section data are presented from 20 to 10⁶ eV for fission and from 30 to 63 eV for the capture-to-fission ratio α . Data in the resonance region (20 to 63 eV) were fitted both by a single-level function consisting of a sum of Breit-Wigner levels and by the Reich-Moore multilevel function based on R -matrix theory. The resulting resonance parameters are listed and discussed. A study of cross sections derived from two and three hypothetical resonances under various conditions of interference is presented to determine the validity of the resonance parameters derived from the multilevel fit.

I. INTRODUCTION

IN June, 1965, neutrons from a nuclear explosion were used for the measurement of the neutron cross sections of several nuclides, including ^{233}U , over the energy range 20 eV to 1 MeV.¹ The details of this

experiment have appeared elsewhere²⁻⁵ and only an outline of the procedure will be given here.

The basic physical design of the experiment (Fig. 1) included the neutron source consisting of a nuclear

* Work performed under the auspices of the U. S. Atomic Energy Commission.

† The work reported here also formed the basis of a dissertation submitted to the University of New Mexico by D. W. Bergen.

¹ D. W. Bergen, M. G. Silbert, and R. C. Perisho, in CONF-660303, 1966, p. 895 (unpublished).

² P. A. Seeger, A. Hemmendinger, and B. C. Diven, *Nucl. Phys.* **A96**, 605 (1967).

³ A. Hemmendinger *et al.*, Los Alamos Scientific Laboratory Report No. LA-3478, Part I (unpublished).

⁴ P. A. Seeger and D. W. Bergen, Los Alamos Scientific Laboratory Report No. LA-3478, 1966, Part II (unpublished).

⁵ D. W. Bergen, Los Alamos Scientific Laboratory Report No. LA-3476-MS, 1966 (unpublished).

TABLE I. Comparison of average ^{233}U cross section for selected intervals.

| E_1 (eV) | E_2 (eV) | LASL ^a (b) | Moore ^b (b) | Nifenecker ^c (b) | Albert ^{d,e} (b) | James ^f (b) | Perkin ^g (b) | Weston ^h (b) |
|-------------------|-------------------|--------------------------|---------------------------|--------------------------------|------------------------------|---------------------------|----------------------------|----------------------------|
| 20.0 | 27.3 | 182.0 ±14.0 | 83 | 104.1 | | | | 102.2 |
| 27.3 | 38.4 | 87.1 ±7.0 | 43 | 59.3 | | | | 57.6 |
| 38.4 | 51.6 | 41.1 ±3.3 | 23 | 30.0 | 46 | | | 28.2 |
| 51.6 | 66.0 | 67.5 ±5.4 | 34 | | 50 | | | 46.5 |
| 66.0 | 83.7 | 58.4 ±4.6 | 29 | | 35 | | | 39.4 |
| 83.7 | 102. | 48.6 ±3.8 | 27 | | 38 | | | 33.9 |
| 102 | 130 | 53.7 ±4.3 | 32 | | 30 | | | |
| 130 | 159 | 32.8 ±2.6 | 20 | | 28 | | | |
| 159 | 195 | 34.0 ±2.7 | 14 | | 27 | | | 22.6 |
| 195 | 260 | 37.8 ±3.0 | 19 | | 28.5 | | | 25.0 |
| 260 | 320 | 30.6 ±2.4 | 17 | | 32.8 | | | 20.2 |
| 320 | 500 | 23.9 ±1.9 | 14 | | 21 | | | 15.4 |
| 500 | 1.0×10^3 | 20.4 ±1.6 | 12 | | 12.7 | | | 13.6 |
| 1.0×10^3 | 2.0 | 12.4 ±1.0 | | | 10.0 | 9.39 ±0.9 | | |
| 2.0 | 3.0 | 8.62 ±0.69 | | | 7.9 | 7.61 ±0.8 | | |
| 3.0 | 4.0 | 6.83 ±0.55 | | | 6.2 | 5.95 ±0.6 | | |
| 4.0 | 6.0 | 5.25 ±0.42 | | | 6.1 | | | |
| 6.0 | 8.0 | 4.49 ±0.36 | | | 5.2 | 4.80 ±0.4 | | |
| 8.0 | 1.0×10^4 | 4.24 ±0.34 | | | 4.9 | 4.26 ±0.4 | | |
| 1.0×10^4 | 1.5 | 4.28 ±0.34 | | | 4.0 | 3.49 ±0.3 | | |
| 1.5 | 2.0 | 3.78 ±0.30 | | | | | | |
| 2.0 | 3.0 | 3.26 ±0.26 | | | | | 2.73 ±0.11 | |
| 3.0 | 5.0 | 2.81 ±0.22 | | | | | (24 keV) | |
| 5.0 | 1.0×10^5 | 2.23 ±0.18 | | | | | | |
| 1.0×10^5 | 2.0 | 2.18 ±0.18 | | | | | | |
| 2.0 | 4.0 | 2.00 ±0.16 | | | | | | |

^a Errors include statistical errors and the known systematic uncertainty.
^b Reference 9.
^c Reference 8.
^d Interpolated from reported values.

^e Reference 10.
^f Reference 11.
^g Reference 12.
^h Reference 13.

explosion (pulse width $\leq 0.1 \mu\text{sec}$), a moderator near the neutron source to enhance the low-energy neutron flux, a 185-m vertical flight path, and a collimator with 2.9-cm² aperture just beneath the experimental station containing the target foils. Nuclear reactions between the foil atoms and incident neutrons were observed by semiconductor detectors. A signal proportional to the ^{233}U fission reaction rate was produced by interaction of fission fragments with the detectors. A γ -ray signal proportional to a sum of the fission and capture reaction rates was produced by γ -ray conversion and subsequent electron detection in a Moxon-Rae⁶ system. The neutron flux was so great that individual events could not be observed (typically, hundreds of particles were recorded within the 0.1- μsec resolution time of the electronics); rather, the detector current was converted to a voltage, logarithmically amplified to compress the dynamic range of the signal, and fed to the deflection preamplifier of an oscilloscope. The oscilloscope beam position was recorded as a function of time with a moving-film camera. Since a reference trace containing base-line and timing information was recorded simultaneously on the film, and an amplifier calibration was recorded 5 msec after the neutron signal had died

away, the film records could be converted to a detector signal as a function of time and thence to a cross section by comparing the signal to that from a nuclide of known cross section.

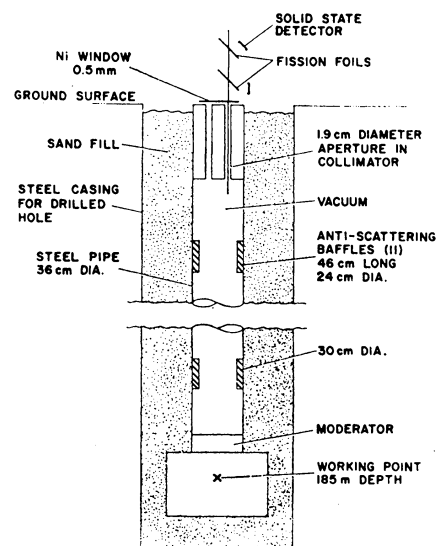


FIG. 1. Schematic diagram showing the basic physical details of the experiment.

⁶ A. Hemmendinger, M. G. Silbert, and A. Moat, IEEE Trans. Nucl. Sci. 12, 304 (1965); M. C. Moxon and R. Rae, Nucl. Instr. Methods 24, 445 (1963).

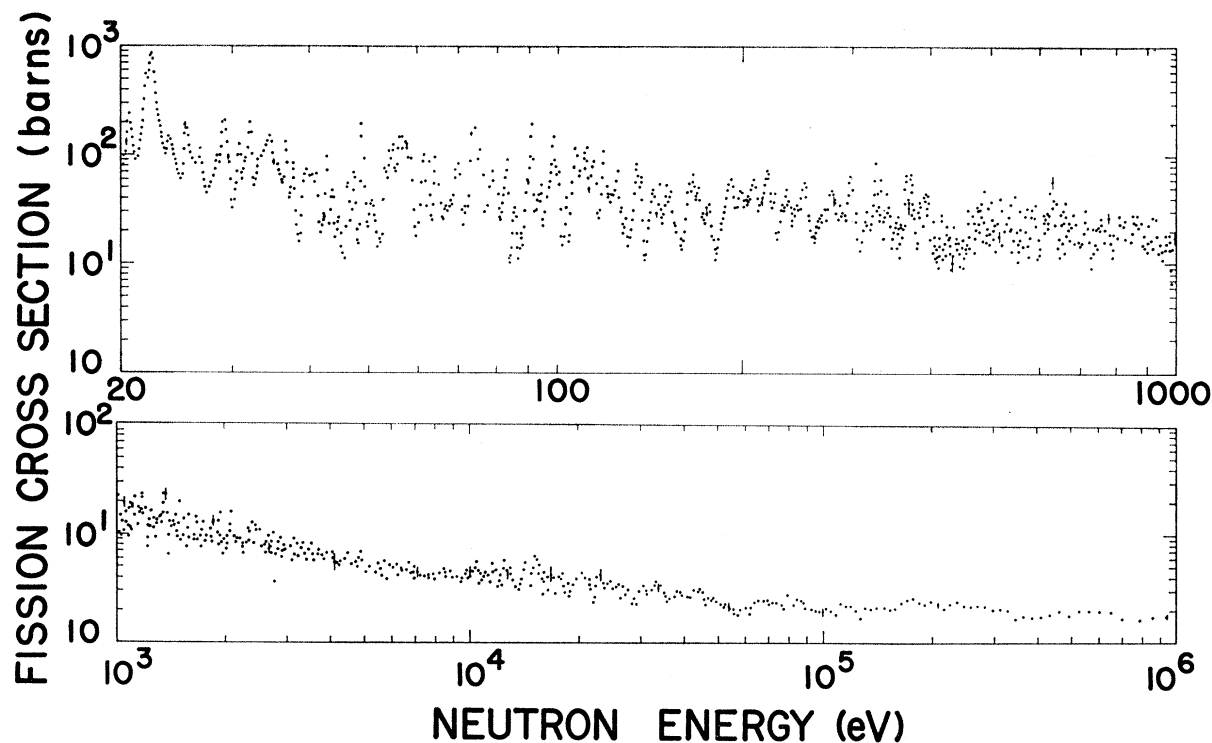


Fig. 2. $^{233}\text{U}(n,f)$ cross section from 20 eV to 10^6 MeV. The points represent the average of the analog signal over time intervals varying from 0.3 μsec at 1 MeV to 2 μsec at 20 eV. All data points are not shown. The error bars shown include all known errors except the 7.9% systematic uncertainty. The small fluctuations above 100 keV are generally within the experimental error. The neutron energy resolution due to the source varied from about 30 keV at 1 MeV to 1.5 eV at 500 eV. For the energies below 100 eV the resolution function is shown in Fig. 5. Reference 5 contains additional information on the neutron source.

Compared to conventional time-of-flight cross-section measurements, this experiment had a very low background; thus, precise measurements were available in valleys between resonances where interference effects between resonances are dominant. An analysis to determine resonance parameters has been performed using both a single-level formalism and an R matrix based multilevel formalism, and results of these two analyses are compared.

II. SAMPLE PREPARATION

The 4-cm-diam ^{233}U fission foil was prepared by vacuum evaporation of UO_2 onto a 0.006-mm thick Pt backing. The foil areal density normal to the neutron beam, as determined by α activity and thermal-fission counting, was $(1.63 \pm 0.05) \times 10^{-6}$ atoms/b. The isotopic composition of the uranium was 97.96% ^{233}U , 1.37% ^{234}U , 0.07% ^{235}U , and 0.60% ^{238}U ; contamination corrections were not made in computing cross sections.

The ^{233}U capture foil was a 4-cm-diam disk of U metal encapsulated in a 0.25-mm thick aluminum case.

The foil areal density as determined by geometry and weight was $(1.67 \pm 0.08) \times 10^{-8}$ atoms/b, composed of 97.79% ^{233}U , 1.49% ^{234}U , 0.09% ^{235}U , and 0.63% ^{238}U .

III. RESULTS

The ^{233}U fission cross sections shown in Figs. 2 and 3 were determined relative to the ^{235}U fission cross section⁷ above 10 keV and to the $^6\text{Li}(n,\alpha t)$ cross section at lower energies. As an intercomparison, the flux derived from ^6Li was used to calculate σ_f for ^{235}U below 10 keV. The resultant ^{235}U cross sections agree well with those of previous measurements.⁷

A comparison of ^{233}U results with those of other measurements⁸⁻¹³ is shown in Table I. The errors listed with the current measurement include a 7.9% systematic uncertainty in the geometry and areal densities of the ^{233}U , neutron flux, and background. The number of recorded fissions represented by each datum point shown in Fig. 2 ranged from greater than 20 000 at both 50 eV and 1 MeV to a minimum of a few hundred

⁷ Staff Report, Los Alamos Scientific Laboratory Report No. LA-3586, 1966 (unpublished).

⁸ H. Nifenecker, D. Paya, and J. Fagot, *J. Phys. (Paris)* **24**, 254 (1963).

⁹ M. S. Moore, L. G. Miller, and O. D. Simpson, *Phys. Rev.* **118**, 714 (1960).

¹⁰ R. D. Albert, *Phys. Rev.* **142**, 778 (1966).

¹¹ G. D. James, in *Proceedings of the International Conference on Fast Critical Experiments and Their Analysis*, 1966 (unpublished).

¹² J. L. Perkin *et al.*, *J. Nucl. Energy: Pt. AB*, **19**, 423 (1965).

¹³ L. W. Weston *et al.*, Oak Ridge National Laboratory Report No. ORNL-TM-1751, 1967 (unpublished).

at 1 keV. The random errors which appear on every 50th point in the figures include the greater of the uncertainties of the film trace readings (including calibrations) or the statistical error in the number of fragments detected,⁴ but do not include the systematic 7.9% error mentioned above. Figure 2 demonstrates the cross-section fluctuations in the intermediate energy range 1.0 to 2.0 keV.

The energy scale was determined by an accurate measurement of the flight path and the neutron pulse time as established by the associated source γ rays. The scale was checked by observation of known resonances in ^{235}U , ^{240}Pu , and Pt. A crystal-controlled oscillator provided timing information along the length of the film.

The structure in our cross section agrees quite well with that observed by Nifenecker⁸ and Weston *et al.*¹³; however, although the cross sections are in substantial agreement with previous measurements above 100 keV, the present data fall above those of all other measurements over most of the energy range. The normalization factors required to bring about agreement with other data are: (1) 0.8, to agree with Perkin's data, and (2) 0.69, to agree with Weston's data from 1 keV to 27 eV, decreasing to 0.56 over the 22.4-eV resonance. Our energy scale agrees with that of Weston, but a shift is required to achieve agreement with Nifenecker's data.

Since other cross sections measured on the same experiment do not exhibit this normalization problem, any error in the ^{233}U cross section would necessarily be associated with the detector-amplifier-recording system used with the ^{233}U . A satisfactory reason for this discrepancy in the absolute value of the fission cross section has not been found to date. A complete listing of the $^{233}\text{U}(n,f)$ cross sections with the associated errors is given in Ref. 7.

The capture-plus-fission cross section was measured by recording the fission and capture γ rays from the capture sample. Since thick samples of Pt and ^{240}Pu were in the neutron beam between the source and the thick ^{233}U capture sample, the flux was substan-

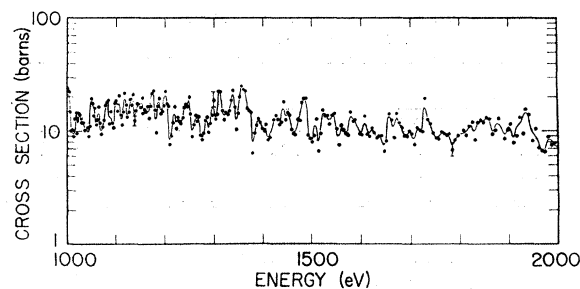


FIG. 3. The ^{233}U fission cross section from 1 to 2 keV, showing the fluctuation in σ_f . The line represents a two-point running average.

tially reduced at each Pt or ^{240}Pu resonance, rendering impossible an accurate measurement of the cross section in the vicinity of these resonances. The capture-to-fission ratio α , displayed in Figs. 4(a) and 4(b) over the energy range 30 to 63 eV, therefore has gaps at 38 and 42 eV due to ^{240}Pu resonances. Because of uncertainty in the detector efficiency for fission and capture γ 's, the capture-plus-fission signal was normalized to the fission data at a broad peak at 34 eV, where the cross section was assumed to be mostly fission. The value of $\sigma_f + \sigma_c$ at this point was assumed to be 1.077 times the fission cross section. The α data are displayed only for comparison to the multilevel and single-level fits, and absolute error assignments have not been made to the data. Such errors include the relative efficiency of the detector to capture and to fission, the uncertainty in the normalization, the statistical error, the small effect of multiple scattering in the target, and (as it applies to the thick target correction made on the capture data) the error in the absolute-fission cross section. The average value for α over the energy interval 30–63 eV is 0.187.

IV. DATA ANALYSIS

Theoretical fits have been made previously to the ^{233}U cross sections, using both single and multilevel

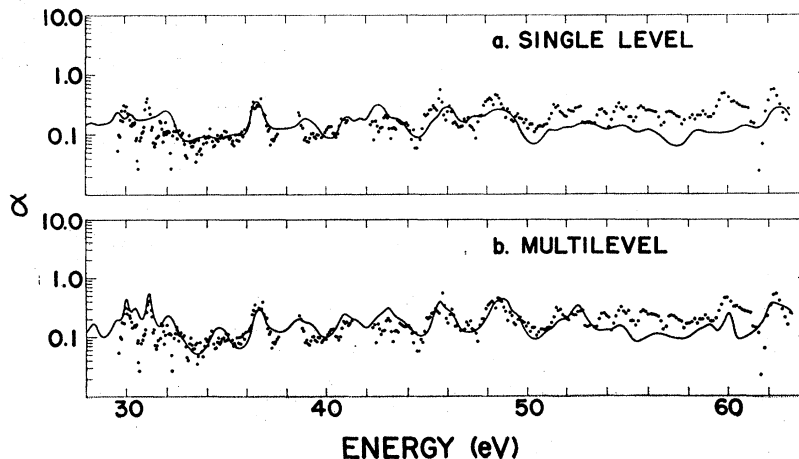


FIG. 4. (a) The measured ^{233}U α (points) compared to the α computed from the single-level fitting parameters. (b) The measured ^{233}U α compared to the α computed from the multilevel parameters.

TABLE II. The probability of "unmixed" resonances—2-channel case.

| $\langle\Gamma_1\rangle/\langle\Gamma_2\rangle$ | $P(1/10)$ | $P(1/5)$ | $P(1/3)$ | $P(1/2)$ |
|---|-----------|----------|----------|----------|
| 0.2 | 0.51 | 0.68 | 0.84 | 1.0 |
| 0.5 | 0.44 | 0.62 | 0.80 | 1.0 |
| 1.0 | 0.43 | 0.60 | 0.79 | 1.0 |

formalisms (0–10 eV multilevel,¹⁴ 0–40 eV single level¹⁵). In order to compare these two approaches, and simultaneously gain some insight into the effect of interference between levels, both single and multilevel fits have been made to the present ²³³U data between 20 and 63 eV; the experimental resolution did not warrant fitting to higher energies. It is likely that, because of the many-channel nature of the capture reaction, the capture cross section would be influenced very little by interference. Peaks in the fission cross section produced by cooperative interference would then show a very low capture-to-fission ratio α , and this ratio would increase sharply in deep fission valleys caused by destructive interference. With this in mind, the α data from this experiment were used as a measure of the validity of the fit; the fits were performed solely on the fission data and the resulting resonance parameters were used to compute the α shown compared to the experimental data in Figs. 4(a) and 4(b). The relatively weak variation in α as measured and shown in the fit confirms the observation by Nifenecker¹⁵ that interference effects appear weak for ²³³U fission.

A sum of Breit-Wigner levels,¹⁶

$$\sigma_f(E) = \pi\lambda^2 g \sum_j \{ \Gamma_{nj} \Gamma_{fj} / [(E_j - E)^2 + \frac{1}{4}\Gamma_j^2] \},$$

was used for the single-level fit. The multilevel fit employed equations based on the Wigner-Eisenbud formalism¹⁷ developed for computation by Reich and Moore¹⁸; in this formalism, the fission cross section takes the form¹⁹

$$\sigma_{1f} = \sum_{n=2}^{l+1} 4\pi\lambda_1^2 g_1 | (1-K)_{1n}^{-1} |^2,$$

where the subscript 1 refers to the neutron entrance channel; the elements of K form an $(l+1) \times (l+1)$ matrix from the neutron channel and the l fission channels. The elements of K are

$$K_{ij} = \frac{1}{2}i \sum_{\lambda} [\Gamma_{i\lambda}^{1/2} \Gamma_{j\lambda}^{1/2} / (E_{\lambda} - E - \frac{1}{2}i\Gamma_{\gamma\lambda})].$$

The cross sections computed from these equations were

¹⁴ M. S. Moore and C. W. Reich, Phys. Rev. **118**, 718 (1960).

¹⁵ H. Nifenecker and G. Perrin, in *Proceedings of the Symposium on Physics and Chemistry of Fission* (International Atomic Energy Agency, Vienna, 1965), p. 245.

¹⁶ G. Breit and E. P. Wigner, Phys. Rev. **49**, 519 (1936).

¹⁷ E. P. Wigner and L. Eisenbud, Phys. Rev. **72**, 29 (1947).

¹⁸ C. W. Reich and M. S. Moore, Phys. Rev. **111**, 929 (1958).

¹⁹ D. R. Harris, p. 823 of Ref. 1.

convoluted with the Doppler and resolution functions by numerical integration before they were compared to the experimental cross sections. The resolution function shown in Fig. 5 was determined from the shapes of narrow resonances in ²⁴⁰Pu and is essentially that expected from the moderator.²

V. INTERPRETATION OF RESULTS

1. Fitting Considerations

The nuclide ²³³U has ground-state spin and parity $I^{\pi} = \frac{5}{2}^{+}$; therefore, the ²³⁴U compound nucleus formed by s -wave neutron capture will have J^{π} of 2^{+} or 3^{+} . A fission threshold appears to lie about 1.4 MeV below the energy of the ²³⁴U compound nucleus produced by zero-energy neutrons, and a second fission threshold falls some 0.7 MeV higher.²⁰ According to the scheme of Wheeler²¹ as extended by Lynn,²² the first threshold is most likely a 2^{+} rotational state built on the ²³⁴U ground-state configuration, while the second is due to a one-quantum γ vibration (producing 2^{+} states) with rotational energy (3^{+} states). Finally, at a somewhat higher energy (perhaps near the energy of the compound nucleus), a mixed state of one quantum shape deformation and one quantum bending (2^{+}) with rotational energy (3^{+}) will occur. One would therefore expect at least two fission channels to contribute to the 2^{+} resonance widths and one to the 3^{+} resonances.

With this in mind, the fission data were fitted, assuming three fission channels, under the restriction that each resonance was assigned to only one channel. This restriction may introduce two errors: (a) resonances belonging to a given spin state and fission channel are strongly affected by interference with other resonances whose primary fission width is in the same fission channel²³; (b) resonances in a spin state with more than one contributing channel will in general have partial widths in all channels. If two channels of average

²⁰ J. A. Northrup, R. H. Stokes, and K. Boyer, Phys. Rev. **115**, 1277 (1959).

²¹ John A. Wheeler, in *Fast Neutron Physics*, edited by J. L. Fowler and J. B. Marion (Interscience Publishers, Inc., New York, 1963), Vol. II, p. 2051.

²² J. E. Lynn, in *Proceedings of the International Conference on the Study of Nuclear Structure with Neutrons*, edited by M. Nève de Mévergnies, P. Van Assche, and J. Vervier (North-Holland Publishing Co., Amsterdam, 1966), p. 441.

²³ Resonances in separate channels of similar spin also interfere weakly through the neutron channel. This interference is negligible, as can be seen from the cross section calculated to first order in Γ_n/Γ_t using the Reich-Moore formalism for the case of two fission channels, each containing a single isolated resonance:

$$\sigma_f(E) \cong \pi\lambda^2 \left\{ \sum_{k=1, j \neq k}^2 \frac{\Gamma_{kn} \Gamma_{kf}}{(E_k - E)^2 + \frac{1}{4}\Gamma_k^2} \times \left| \frac{1}{1 - \frac{1}{2}i[\Gamma_{jn}/E_j - E - \frac{1}{2}i(\Gamma_{j\gamma} + \Gamma_{jf})]} \right|^2 \right\},$$

where Γ_{kn} , Γ_{kf} , $\Gamma_{k\gamma}$, and Γ_{kt} are the partial neutron, fission, capture, and total widths, respectively, for the k th resonance. For the usual case, Γ_{kn} is much less than $\Gamma_t + |E - E_k|$ and the corrective term is negligible.

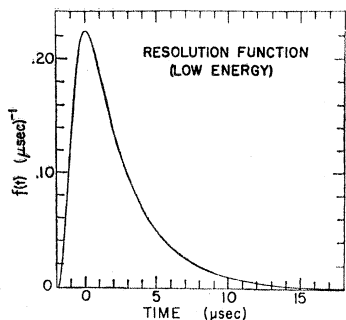


FIG. 5. The resolution function used in the fitting computation. The area under the curve has been normalized to unity.

fission widths $\langle\Gamma_1\rangle$ and $\langle\Gamma_2\rangle$ are open in a given spin state, the probability of a resonance having the fraction R , or less, of its fission width in one channel is given (assuming the width distribution each to obey Porter-Thomas distributions of one degree of freedom) by

$$P(R) = 1 - \frac{1}{2\pi} \int_0^\infty dy \int_a^b \frac{dx}{(xy)^{1/2}} e^{-(1/2)(x+y)},$$

with $a = \gamma[R/(1-R)]\langle\Gamma_1\rangle/\langle\Gamma_2\rangle$, $b = \gamma[(1-R)/R]$

TABLE III. Single-level resonance parameters.

| Energy (eV) | $2g\Gamma_n^0$ (meV) | Γ_f (meV) | Γ_γ (meV) | Energy (eV) | $2g\Gamma_n^0$ (meV) | Γ_f (meV) | Γ_γ (meV) |
|-------------|----------------------|------------------|-----------------------|-------------|----------------------|------------------|-----------------------|
| 20.58 | 0.38 | 360 | 45 | 39.32 | 0.056 | 250 | 45 |
| 21.88 | 0.53 | 200 | | 39.56 | 0.055 | 250 | |
| 22.36 | 1.51 | 350 | | 39.89 | 0.145 | 600 | |
| 22.96 | 0.18 | 450 | | 40.49 | 0.175 | 650 | |
| 23.78 | 0.22 | 390 | | 41.06 | 0.091 | 190 | |
| 24.26 | 0.105 | 530 | | 41.75 | 0.009 | 150 | |
| 24.64 | 0.01 | 200 | | 42.16 | 0.035 | 350 | |
| 25.27 | 0.30 | 260 | | 42.66 | 0.19 | 140 | |
| 25.75 | 0.10 | 340 | | 43.53 | 0.093 | 240 | |
| 26.08 | 0.05 | 200 | | 44.58 | 0.086 | 660 | |
| 26.30 | 0.035 | 100 | | 45.38 | 0.006 | 180 | |
| 26.65 | 0.17 | 300 | | 46.16 | 0.105 | 150 | |
| 27.05 | 0.015 | 200 | | 46.71 | 0.01 | 200 | |
| 27.74 | 0.135 | 800 | | 47.05 | 0.075 | 400 | |
| 28.00 | 0.007 | 130 | | 47.36 | 0.13 | 220 | |
| 28.32 | 0.105 | 250 | | 48.76 | 0.445 | 175 | |
| 28.85 | 0.135 | 320 | | 49.30 | 0.050 | 200 | |
| 29.12 | 0.338 | 290 | | 50.48 | 0.184 | 900 | |
| 29.59 | 0.073 | 150 | | 51.23 | 0.021 | 260 | |
| 30.30 | 0.02 | 130 | | 52.06 | 0.016 | 300 | |
| 30.73 | 0.215 | 260 | | 53.17 | 0.19 | 290 | |
| 31.35 | 0.10 | 230 | | 53.54 | 0.055 | 300 | |
| 31.66 | 0.075 | 200 | | 54.15 | 0.30 | 400 | |
| 32.04 | 0.30 | 170 | | 54.89 | 0.33 | 320 | |
| 33.11 | 0.27 | 750 | | 55.81 | 0.23 | 500 | |
| 33.67 | 0.11 | 500 | | 56.18 | 0.20 | 300 | |
| 34.06 | 0.155 | 480 | | 56.58 | 0.34 | 450 | |
| 34.55 | 0.37 | 550 | | 57.55 | 0.74 | 900 | |
| 35.27 | 0.114 | 450 | | 58.54 | 0.23 | 350 | |
| 35.62 | 0.024 | 300 | | 59.35 | 0.009 | 300 | |
| 35.96 | 0.14 | 750 | | 60.38 | 0.045 | 500 | |
| 36.59 | 0.20 | 110 | | 61.07 | 0.08 | 280 | |
| 37.51 | 0.21 | 380 | | 61.50 | 0.36 | 400 | |
| 39.08 | 0.055 | 200 | | 62.72 | 0.29 | 165 | |

^a This parameter should be multiplied by 0.69 if normalized to Nifenecker's or Weston's data.

$\times (\langle\Gamma_1\rangle/\langle\Gamma_2\rangle)$. Table II lists the probability $P(R)$ for various ratios $\langle\Gamma_1\rangle/\langle\Gamma_2\rangle$, and R .

Resonances with $R = \frac{1}{2}$ or less would be difficult to recognize as multichannel; treating these as entirely in one channel should cause little error in the parameters. However, since at least the 2^+ spin-state resonances are expected to have more than one contributing channel, at least 30% of the 2^+ resonances would be affected

TABLE IV. Multilevel resonance parameters.

| Energy ^a (eV) | $2g\Gamma_n^0$ ^b (meV) | Γ_f for the three channels (meV) | Γ_γ (meV) |
|--------------------------|-----------------------------------|---|-----------------------|
| 20.535 | 0.32 | | 40 |
| 21.885 | 0.49 | +190 | 40 |
| 22.33 | 1.34 | -355 | 40 |
| 22.94 | 0.61 | | 65 |
| 23.61 | 0.185 | -540 | 40 |
| 25.245 | 0.25 | | 65 |
| 25.84 | 0.013 | -40 | 40 |
| 26.30 | 0.115 | +550 | 40 |
| 26.63 | 0.19 | -330 | 40 |
| 27.28 | 0.0074 | +250 | 40 |
| 27.69 | 0.14 | | 65 |
| 28.35 | 0.09 | +200 | 40 |
| 29.11 | 0.5 | +420 | 40 |
| 29.55 | 0.105 | +250 | 40 |
| 30.00 | 0.005 | +10 | 40 |
| 30.41 | 0.045 | -200 | 40 |
| 30.72 | 0.235 | +260 | 40 |
| 31.10 | 0.025 | +20 | 40 |
| 31.30 | 0.128 | | 65 |
| 32.06 | 0.27 | -160 | 40 |
| 32.94 | 0.125 | +620 | 40 |
| 34.14 | 0.29 | | 65 |
| 34.64 | 0.37 | -450 | 40 |
| 35.43 | 0.51 | | 65 |
| 36.615 | 0.20 | +120 | 40 |
| 37.505 | 0.198 | +365 | 40 |
| 39.18 | 0.08 | -350 | 40 |
| 39.39 | 0.22 | | 65 |
| 40.83 | 0.126 | | 65 |
| 41.03 | 0.115 | +200 | 40 |
| 41.90 | 0.034 | -460 | 40 |
| 42.69 | 0.21 | -170 | 40 |
| 43.495 | 0.104 | +240 | 40 |
| 44.69 | 0.102 | -690 | 40 |
| 45.50 | 0.011 | -72 | 40 |
| 46.16 | 0.11 | -150 | 40 |
| 47.36 | 0.20 | +385 | 40 |
| 48.79 | 0.49 | +90 | 40 |
| 49.29 | 0.085 | -190 | 40 |
| 50.48 | 0.23 | | 65 |
| 51.25 | 0.036 | +390 | 40 |
| 51.98 | 0.036 | -400 | 40 |
| 52.50 | 0.017 | -240 | 40 |
| 53.16 | 0.29 | | 65 |
| 54.15 | 0.285 | +330 | 40 |
| 54.83 | 0.275 | -260 | 40 |
| 56.16 | 0.305 | +500 | 40 |
| 56.56 | 0.39 | -380 | 40 |
| 57.60 | 0.74 | | 65 |
| 58.59 | 0.21 | +290 | 40 |
| 59.10 | 0.01 | -110 | 40 |
| 60.08 | 0.01 | +20 | 40 |
| 61.62 | 0.45 | | 65 |
| 62.71 | 0.33 | -130 | 40 |

^a Listed energies are those used in the analysis. The absolute energy scale has an uncertainty of less than 0.1 eV at 60 eV and 0.03 eV at 20 eV.
^b This parameter should be multiplied by 0.69 if normalized to Nifenecker's or Weston's data.

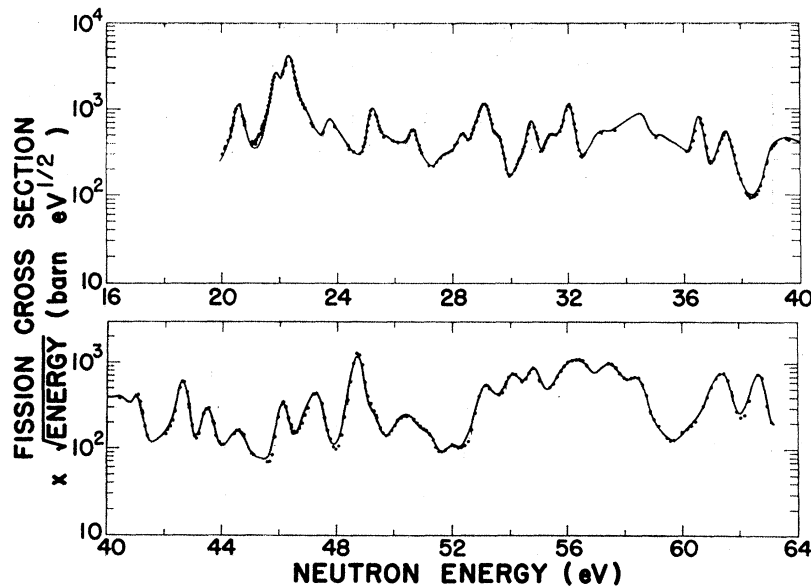


FIG. 6. Single-level fit to the fission data. Data points have been omitted where they lie on the line.

by assuming resonances to fall completely into one channel.

The fixed values for Γ_γ selected in the fits were somewhat arbitrarily chosen. The 45 meV used for the single-level fit was the same value used by Nifenecker.¹⁵ The values used in the multilevel study, 40 meV for channels of smaller $\langle\Gamma_f\rangle$ and 65 meV for the wider $\langle\Gamma_f\rangle$, were guided by Moore's study¹⁴ of a few low-energy ²³⁵U resonances, where some correlation appears between Γ_f and Γ_γ . Because of the relatively wide $\langle\Gamma_f\rangle$ derived from the fit, the choice of Γ_γ is not critical.

2. Resonance Parameters

The fits to the fission data are shown in Figs. 6 and 7 for the single and multilevel analyses, respectively.

The results of the α comparison for both fits appear in Figs. 4(a) and 4(b). As stated earlier, the fits were made to the fission data, then the parameters were used to derive the α shown. It is seen that, while the fission fits are both quite good, the single-level α agrees with the α data only in the region 32–36 eV. The multilevel α agrees with the shape of the α data up to 53 eV. Both fits appear to suffer badly from missed levels at higher energies. Weak fluctuations in Γ_γ from resonance to resonance, not considered here, could also improve the α fits. The multilevel fit included nine fewer resonances than the single-level in the range 30–63 eV, while producing a somewhat better fit. One may conclude from this that, while levels are missed in both fits, many nonexistent resonances are included in the single-level fit.

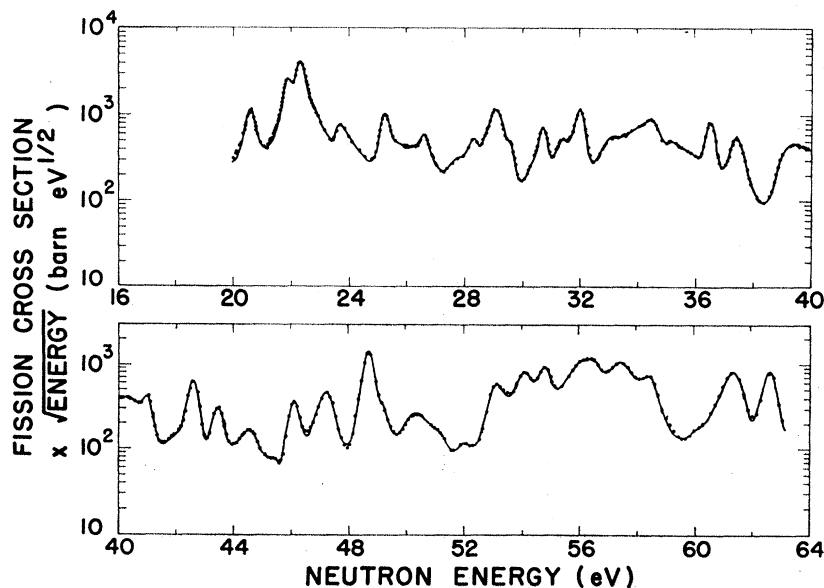


FIG. 7. Multilevel fit to the fission data. Data points have been omitted where they lie on the line.

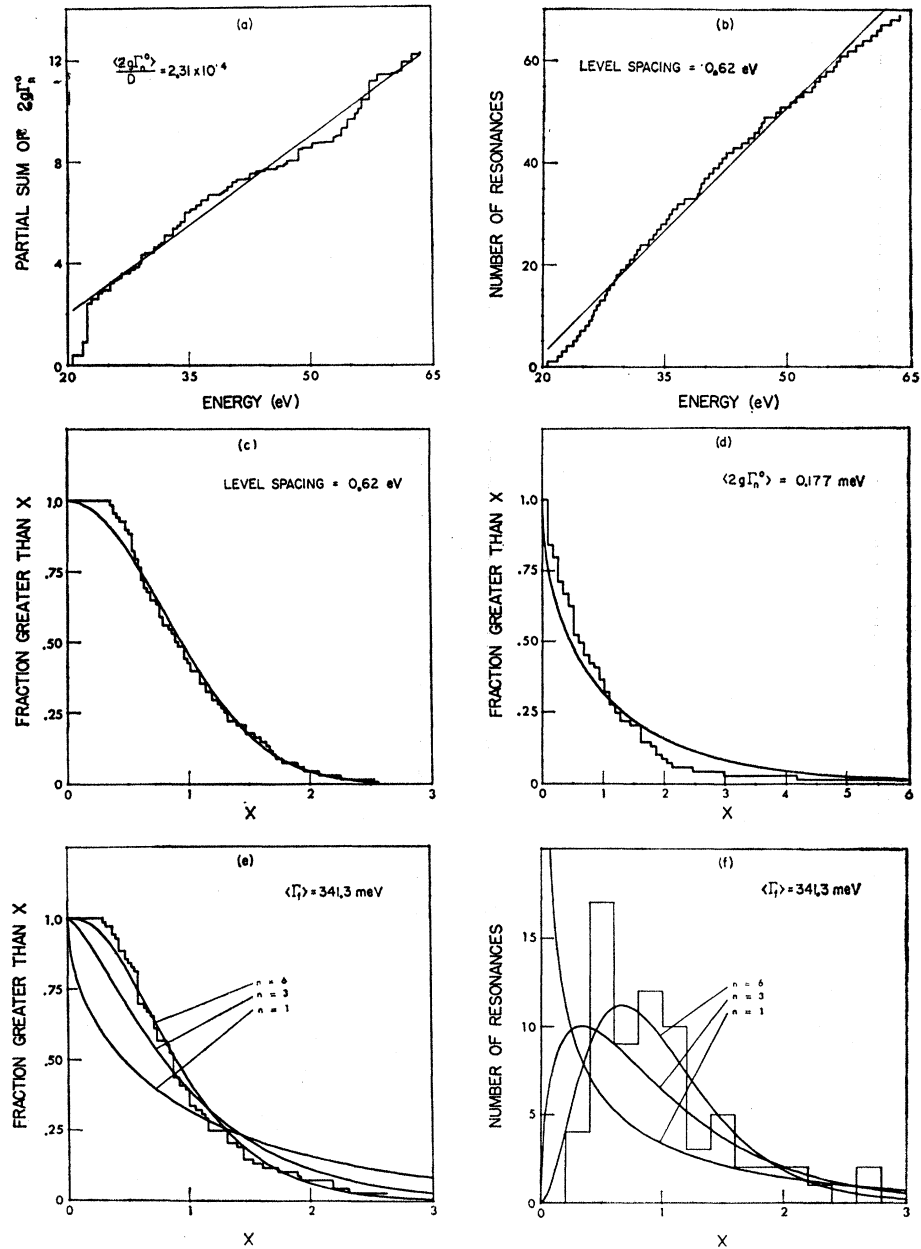


FIG. 8. Single-level resonance-parameter study.

The parameters obtained from the fits are listed in Tables III and IV. Sixty-eight and 54 levels were required for the single-level and multilevel fits, respectively. The reduced number for the multilevel case is a direct result of the added parameter (the sign of the reduced fission width).

Plots of the level density, partial sum of reduced neutron width, reduced neutron width, fission width, and level spacing distributions are shown in Figs. 8 and 9 for the single- and multilevel parameters, respectively. Averages of the spacings and widths are listed on the plots. The "strength function" $S = 2g\Gamma_n^0/D$ listed in (a) of each figure was determined by the least-squares

fit to the data (D is the average spacing of all levels). Both the single-level value, 2.31×10^{-4} , and the multilevel value, 2.39×10^{-4} , compare favorably with that quoted by Nifenecker, 2.09×10^{-4} ,¹⁵ although the fission cross section shown here is about 30% higher than his. Assuming that only levels with small Γ_n^0 have been left out of the fit, S would not be significantly changed by their inclusion; a renormalization of the cross section would, however, change the Γ_n^0 's and S in proportion to the renormalization. The multilevel strength function, when normalized to Weston's¹³ data, becomes 1.7×10^{-4} .

The slight curvature of the level spacing plot—Figs.

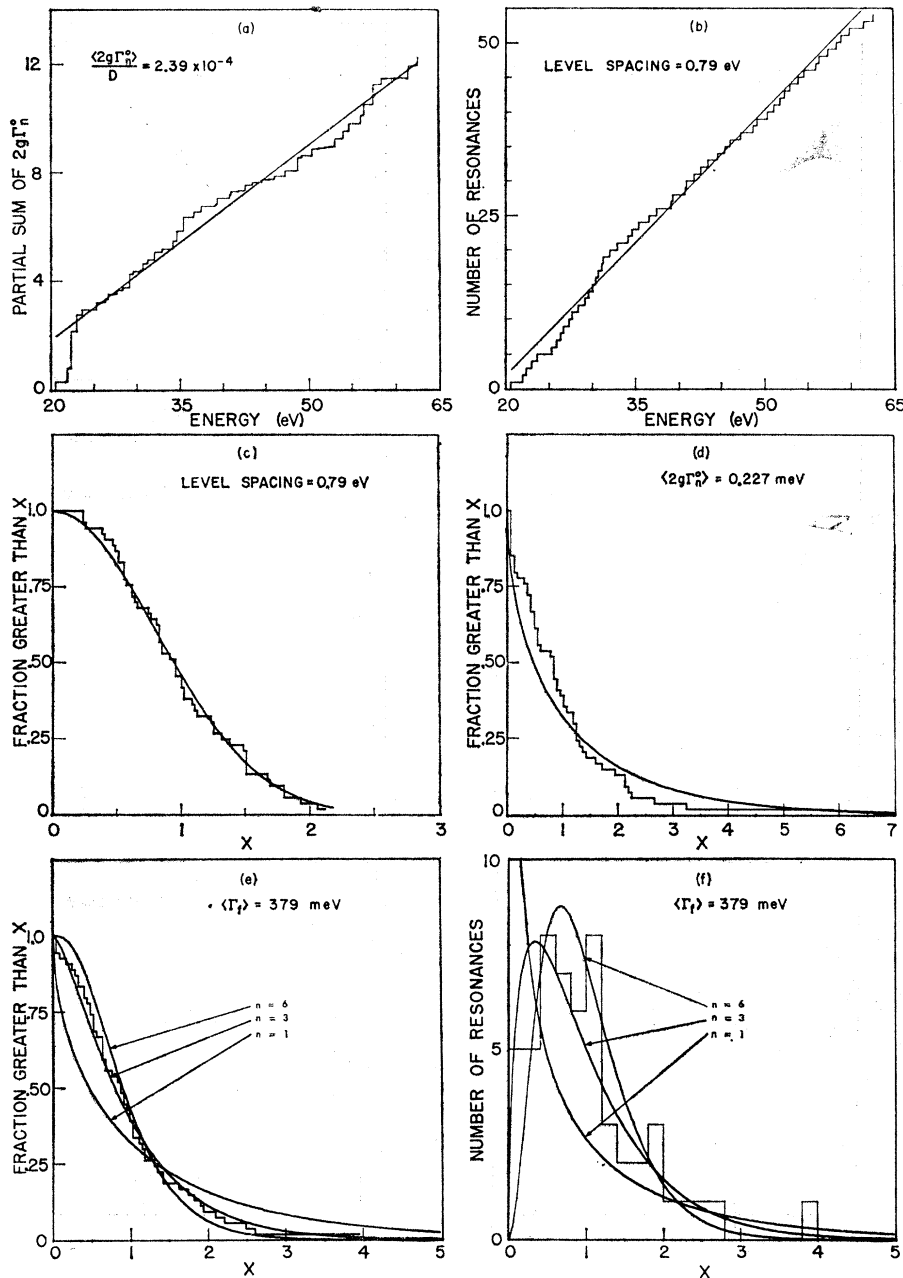


FIG. 9. Multilevel resonance-parameter study.

8(b) and 9(b)—suggests that levels have been overlooked in both fits above 50 eV, due to experimental resolution and Doppler broadening effects. The quoted level spacing was derived from the least-squares line drawn through the data; missed levels would seriously alter these values.

The level-spacing integral histogram, Figs. 8(c) and 9(c), fits the Wigner²⁴ spacing distribution for one family [smooth curve on (c)]. Since the distribution is the result of two families (2^+ and 3^+ states), this agreement, as others have noted,²² is no doubt a result of

closely spaced levels being combined as one. The integral form of the reduced neutron-width histogram is shown in Figs. 8(d) and 9(d) compared to the integral form of the Porter-Thomas²⁵ width distribution for one degree of freedom. This is a valid comparison only if $\langle \Gamma_n^0 \rangle$ is the same in both spin states. The disagreement between the histogram and the curve is most likely due to missing weak levels. The value 0.177 meV for $\langle 2g\Gamma_n^0 \rangle$ obtained from the single-level parameters compares favorably with the value 0.169 meV found by Nifenecker,¹⁵ but a renormalization of the fission data

²⁴ E. P. Wigner, Oak Ridge National Laboratory Report No. ORNL-2309, 1956 (unpublished).

²⁵ C. E. Porter and R. G. Thomas, Phys. Rev. **104**, 483 (1956).

to agree with Nifenecker's data would reduce $\langle 2g\Gamma_n^0 \rangle$ by some 30%. The value 0.227 meV from the multilevel analyses is considerably larger as a result of the reduced number of levels. A 30% adjustment in this number improves the agreement, however.

The integral and differential forms of the fission distributions are shown in Figs. 8(e) and 9(f) respectively. The smooth curves are Porter-Thomas distributions with 1, 3, and 6 degrees of freedom. The values 341 and 379 meV for $\langle \Gamma_f \rangle$ from the single- and multilevel fits, respectively, compare with the value 389 meV found by Nifenecker.¹⁵ The equation

$$\nu = 2\langle \Gamma_f \rangle^2 / (\langle \Gamma_f^2 \rangle - \langle \Gamma_f \rangle^2)$$

yields 6.7 and 3.6 for the number of participating fission channels for the single- and multilevel fits, respectively. The large ν for the single level is due to the large number of artificial resonances of nearly constant Γ_f which have been included in the fit.

3. Effect on the Fission Distribution of Mixing Spin States

Since the fission widths are drawn from two populations (2^+ and 3^+), their distribution will not generally obey the single Porter-Thomas distribution; rather, they should be distributed as

$$P(x)dx = dx \left\{ \left(\frac{1}{2} \nu p x \right)^{\nu/2-1} \frac{e^{-\nu p x/2}}{\Gamma(\frac{1}{2}\nu)} \frac{1}{2} \nu p g_1 + \left(\frac{\mu p x}{2k} \right)^{\mu/2-1} \frac{e^{-\mu p x/2k}}{\Gamma(\frac{1}{2}\mu)} \frac{\mu p}{2k} g_2 \right\},$$

where $p = g_1 + g_2 k$, $k = \langle \Gamma_1 \rangle / \langle \Gamma_2 \rangle$, μ and ν are the effective number of open channels in the respective spin states, and g_1 and g_2 are the fraction of levels belonging to each state.

Since, within a given spin state, fission may occur through any of several channels, each with a probability related to the energy by which the excitation energy exceeds the channel threshold, the χ^2 parameter for the number of degrees of freedom which best fits the distribution of widths will in general be proportional to, but less than, the number of participating channels. Thus ν and μ in the above equation would each assume any number equal to or greater than 1. Combining the parameters from the two states produces a distribution which, when compared to a Porter-Thomas distribution, is in most cases fitted best with fewer degrees of freedom than the number of participating channels in either spin state (assuming $\langle \Gamma_f \rangle$ to be different for each state).

The effect of missed levels further complicates estimating the number of open channels within each state. The effect of selective omission of resonances with very small and very large Γ_f 's would probably dominate the calculated number of open channels. An effort was made to estimate the number of missed levels for ^{233}U by creating a mock cross section based on the average

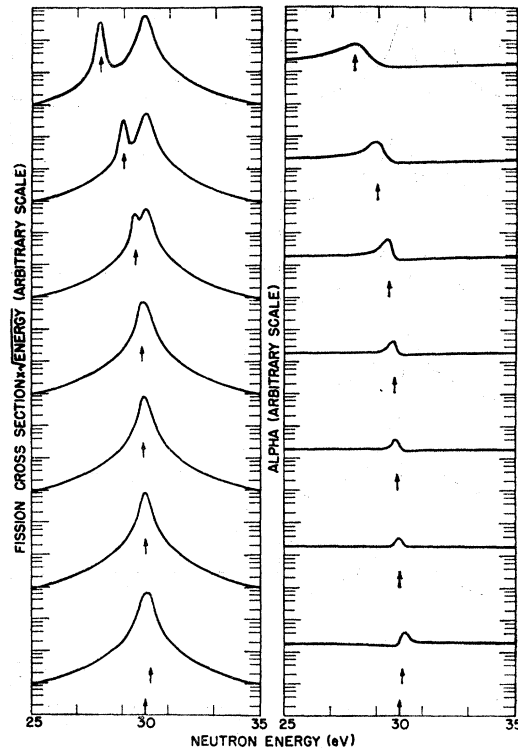


FIG. 10. Two-resonance study showing $\sigma E^{1/2}$ and α . The values were derived using the single-level equation.

values from the multilevel fit, using the technique discussed by Moore,²⁶ and comparing the number of maxima in the mock data to the number of resonances. Applying this comparison to the ^{233}U , about 30% of all resonances were overlooked in the fit. The unobserved resonances in the mock data were primarily weak (small Γ_n^0); however, a few cases of Lynn doublets²² caused resonances to be overlooked in the mock data. Additional work is under way to study some of the effects set forth by Lynn,²² along with the effect of missed levels on the resonance parameters, by creating and fitting mock cross-section data using the Reich-Moore formalism.

Since the α data shown here and the results of Weston¹³ give no evidence of levels in the capture data which do not appear in the fission data, one may assume that very small Γ_f 's have a low probability of occurring. If the distribution of widths obeys a Porter-Thomas distribution, this can be true only if at least three channels each of average width similar to or greater than $\langle \Gamma_f \rangle$ participate in fission in each spin state.

VI. MULTILEVEL CROSS-SECTION INTERPRETATION

Concerning the validity of the resonance parameters and therefore the usefulness of fitting fission data with the currently available multilevel equations, this

²⁶ M. S. Moore and O. D. Simpson, p. 840 of Ref. 1.

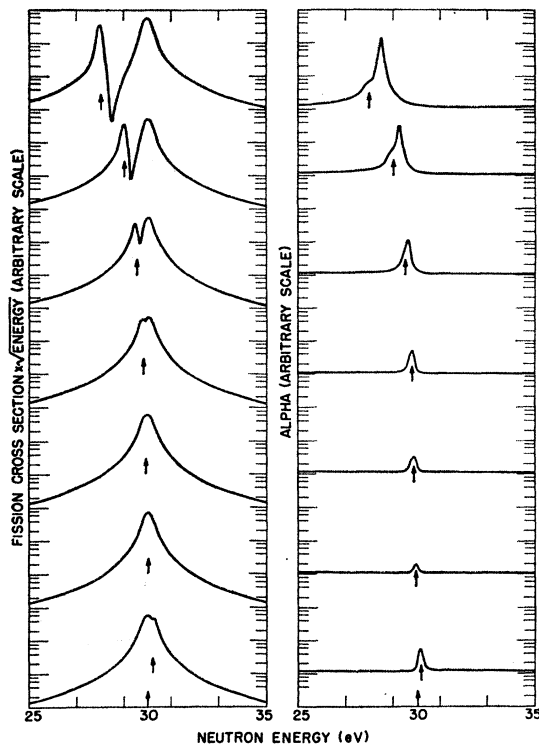


FIG. 11. Multilevel resonance study showing $\sigma E^{1/2}$ and α . The sign of $\Gamma_f^{1/2}$ was the same for both resonances.

section is devoted to the physical results which one might derive from the Reich-Moore formalism.

Lynn²² demonstrated clearly the difficulties associated with interpreting the cross section resulting from two levels of different widths lying quite close together. A similar study has been carried out here for both two and three levels, which indicates that the presence of close-lying levels may be established with the aid of α data, as a consequence of the few-channel nature of fission. For the two-level case, resonances were chosen with parameters, $\Gamma_\gamma = 40$ meV, $\Gamma_{f1} = 60$ meV, $\Gamma_{f2} = 300$ meV, $\Gamma_{n1}^0 = 0.09$ meV, and $\Gamma_{n2}^0 = 0.2$ meV. The energy of the second resonance was held fixed at 30 eV, while the first resonance was moved past it. The separations were chosen at 2, 1, 0.5, 0.2, 0.1, 0 and -0.2 eV. The results of both the fission cross section and the capture-to-fission ratio α are shown in Fig. 10 (single level), Fig. 11 (multilevel with the signs of $\Gamma_f^{1/2}$ both positive), and Fig. 12 (multilevel with opposite signs on $\Gamma_f^{1/2}$). The arrows shown on each figure mark the location of the narrow resonance; the position of the broad resonance is marked with a single arrow at the base of the figure.

The curves have been Doppler-broadened, assuming a temperature of 300°K; resolution broadening was not performed. The variations in α are quite spectacular and leave little doubt in the position and relative sign of the two resonances, although in the case of near superposition the levels always appear as one. The value of α on the right-hand edge of each graph is approx-

imately 0.2 (Fig. 10), 0.1 (Fig. 11), and $\sim 0.3-0.4$ (Fig. 12). The single-level case describes the situation for levels in different spin states or channels; even here, with near superposition (a much more probable situation than for the resonances from the same spin state) the α data indicate clearly the presence of the two levels. This variation of course becomes small for a weak level in the presence of additional levels, or as the ratio Γ_{f1}/Γ_{f2} approaches unity.

The rather strong effect of interference on α is again shown in Fig. 13, where the case of a weak level ($\Gamma_n^0 = 0.02$ meV) on the flank of a strong resonance ($\Gamma_n^0 = 0.2$ meV) is considered ($\Gamma_f = 300$ meV and $\Gamma_\gamma = 40$ meV for both resonances). The stronger resonance was placed at 30 eV in all cases, with the weaker resonances placed either at 29.5 or 29.9 eV. All relative signs of the reduced fission width are considered (see the symbol at the location of the weak resonance in Fig. 13). The sign of $\Gamma_f^{1/2}$ for the larger resonance was always taken to be positive.

The three-level case with Doppler broadening was also considered and is shown in Fig. 14. The parameters used are listed in Table V. Five cases were considered, including the single-level analysis (lower curves) and all possible relative signs of the reduced fission widths (see symbols shown on each of the upper four curves) for the multilevel analyses.

Again, all cases except the single-level treatment are unambiguously determined by combining the α data

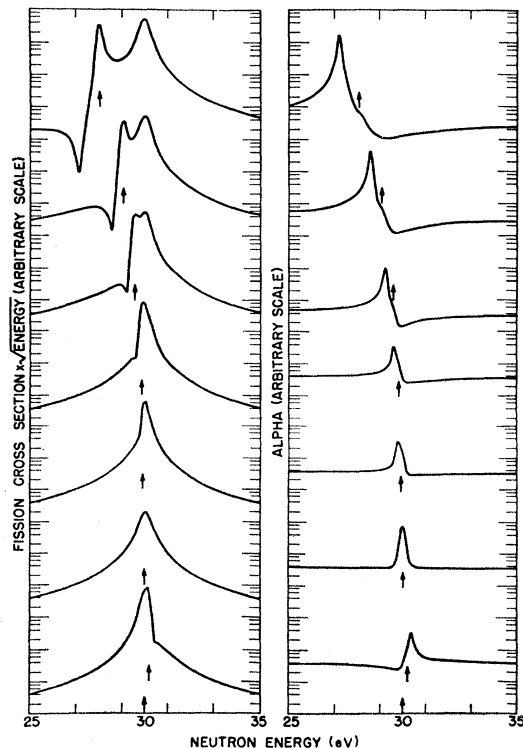


FIG. 12. Multilevel resonance study showing $\sigma E^{1/2}$ and α . Opposing signs were given to $\Gamma_f^{1/2}$ for each resonance.

TABLE V. Parameters for three-resonance study.

| Resonance | E_i (eV) | Γ_n^0 (meV) | Γ_f (meV) | Γ_γ (meV) |
|-----------|---------------|-----------------------|---------------------|--------------------------|
| 1 | 29.2 | 0.230 | 340.0 | 45.0 |
| 2 | 30.0 | 0.230 | 340.0 | 45.0 |
| 3 | 30.8 | 0.230 | 340.0 | 45.0 |

with the fission results. The rather dramatic change in the average value of α for each curve should also be noted. These results suggest that the simultaneous measurement of fission and capture cross sections could be interpreted by R -matrix formalism for cases where only one or two channels per spin state are open for fission.

VII. SUMMARY

The fission data presented here demonstrate the resolution available using the nuclear-detonation neutron source; also to be noted is the accurate energy scale resulting from the precisely measured flight path and time reference provided by the γ -ray flash and crystal-controlled oscillator. The accuracy of the energy scale is easily cross-checked by comparing the energy of resonances occurring in other samples exposed in the same beam to previous measurements.⁷ The ^{238}U fission cross section, although defining accurately the resonance wing and valley shapes, is higher than previous measurements by a systematic factor. The source of this normal-

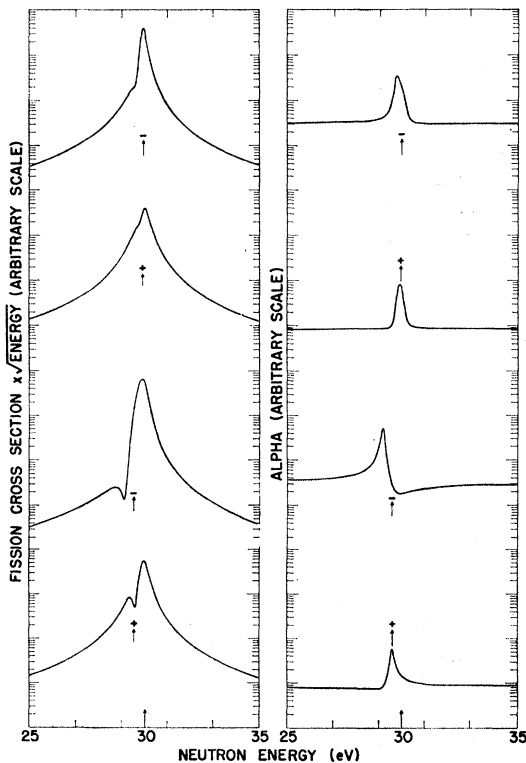


FIG. 13. Multilevel resonance study showing $\sigma E^{1/2}$ and α for the case of a weak resonance on the wing of a strong resonance.

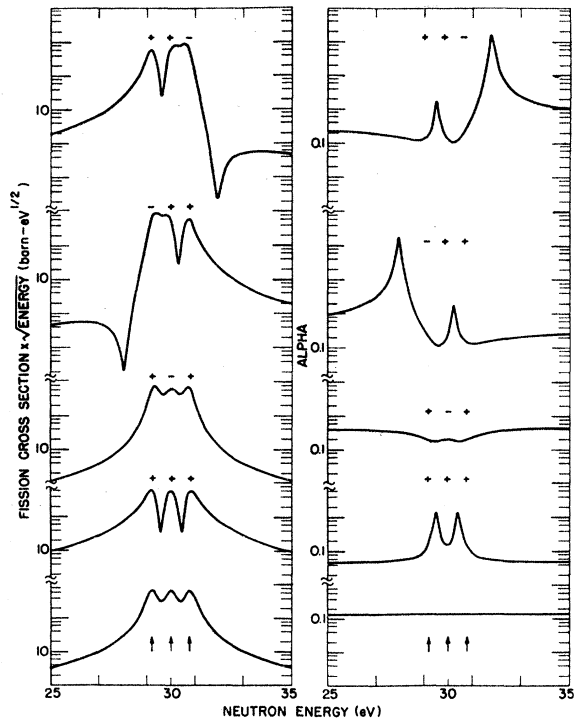


FIG. 14. Three-resonance study showing $\sigma E^{1/2}$ and α for the single-level equation (lower curves) and the multilevel equation. The relative sign for $\Gamma_f^{1/2}$ is shown above each curve.

ization discrepancy is unknown. The average value obtained for α in the region 30 to 63 eV, 0.187, is considerably lower than that observed for ^{239}Pu and ^{235}U .

In an experiment such as the one under discussion, in which the cross sections from two spin states are superimposed on one set of data, attempts to determine the number of channels participating in the fission process in each state are fraught with difficulty. The fluctuation in α might well be a valid way to estimate this number and the weak fluctuation of α for ^{238}U indicates that interference effects are weak and, thus, that several channels are participating in fission. We have concluded that at least three channels, each of average fission width comparable to $\langle \Gamma_\gamma \rangle$, must be open in each spin state. This estimate is based on the fission width distributions [Figs. 9(e) and 9(f)], the weak fluctuations in α , and the lack of very small fission widths as determined from the capture data.

ACKNOWLEDGMENTS

We are indebted to the many colleagues who participated in the nuclear-explosion-cross-section experiments. These include the LASL personnel under the joint leadership of A. Hemmendinger and B. Diven, the LASL Test Division, and the Idaho Nuclear Corporation, Nuclear Cross Sections Group.

We also thank J. Povelites for preparing the ^{238}U fission foil and F. Jones for performing the isotopic analyses of the foils.